

An Investigation to Nonlinear Elastic Behavior of Pericardium Using Uniaxial Tensile Test

M. Arman, K. Narooei*

Department of Materials Science and Engineering, K. N. Toosi University of Technology, Tehran, Iran.

Article info

Article history:

Received 2016.04.06

Received in revised form
2016.06.11

Accepted 2016.06.21

Keywords:

pericardium
nonlinear elastic behavior
strain energy function
Green material
Cauchy material

Abstract

In this paper, the nonlinear elastic behavior of pericardium of human, canine, calf and ostrich was studied. For this purpose, the mechanical behavior was investigated from two viewpoints of the Cauchy and Green elastic materials. Firstly, the experimental data were fitted by Cauchy elastic stress equation. The results showed that the response of Cauchy elastic materials was not fitted with the experimental data appropriately. Secondly, the Green elastic materials were studied by assuming strain energy functions for the mechanical response of the samples. For this purpose, the exponential-exponential, power law-power law, and exponential-power law energy functions were investigated by mathematical programming. It was observed that all energy functions were fitted with the experimental data accurately, especially the power law-power law function. Finally, it was observed that the Green elastic materials theory was more appropriate for studying the mechanical behavior of pericardium by comparing the experimental and theoretical results.

1. Introduction

Pericardium is a tough double layered membrane covering the heart. It plays an important role in the normal cardiac work. Its major functions include: maintenance of adequate cardiac position, separation from the surrounding tissue of the mediastinum, protection against ventricular dilatation, maintenance of low transmural pressure, facilitation of ventricular interdependence and arterial filling. Given the position and role of pericardium, it is necessary to study the behavior of it in the face of environmental factors. Noort et al. introduced a new experimental technique to study the effects of glutaraldehyde and formaldehyde on the stress-strain response of bovine pericardium [1]. Also, Chew et al. investigated canine pericardium behavior under biaxial loading conditions using a new quantitative method [2]. Maestro et al. compared the mechanical and chemical behavior of glutaraldehyde-preserved ostrich pericardium as a novel biomaterial with bovine pericardium, observing that the tensile strength of os-

trich pericardium was higher than bovine pericardium [3]. Daar et al. investigated the effects of penetrating ionising photon radiation on the mechanical properties of pericardium in the uniaxial tensile test. In this research, it was concluded that UTS was reduced to the dose of 80 Gy [4]. Paez et al. studied the mechanical behavior of calf, pig, and ostrich pericardium in unsutured and sutured states using a statistical method; it was concluded that ostrich pericardium had suitable mechanical resistance, relative to pig and calf pericardium, and it could be used as new biomaterials in the fabrication of bioprosthesis [5]. Claramunt et al. studied the fatigue behavior of young ostrich pericardium and presented the relationship between the number of cycles until the failure of each sample and the maximum pressure by the least square method [6]. Cohn et al. compared the mechanical behavior of canine, human, and bovine isolated pericardium in tensile testing [7]. Zioupos and Barbenel, on the other hand, proposed a constitutive law for the investigation of the mechanical behavior of native bovine pericardium in

*Corresponding author: Keivan Narooei (Assistant Professor)
E-mail address: knarooei@kntu.ac.ir

uniaxial and biaxial tensile tests [8]. Lee and Boughner conducted uniaxial tensile tests on the human and canine pericardium tissue to compare the viscoelastic response, showing that the human pericardium, in contrast to canine pericardium, indicated a greater viscous behavior [9]. Gundiah et al. studied the strain energy functions (SFE) for arterial elastin and concluded that Mooney-Rivlin model did not cover the arterial elastin behavior. Thus, they proposed an orthotropic materials model [10]. Zulliger et al. proposed a new SFE by expanding the model developed by Fung and Holzapfel model, characterizing the fraction of both elastin and collagen on rat carotids [11]. Also, Zulliger and Stergiopoulos studied the main structural factors of the human thoracic aorta using the strain energy function. In this research, it was shown that the changes in the mechanical behaviour of aorta could not be included in the elastic constants of elastin and collagen by increasing the age [12]. Kulkarni et al. studied the bovine pericardium and porcine brain tissue using transversely hyperelastic materials including matrix and reinforced fibres, by considering the large deformation at high strain rates. The matrix part was simulated using the Neo-Hookean strain energy function and in the fibres part, the polyconvex polynomial model was used [13]. Pavan et al. presented a constitutive model considering the incompressibility, large strain and time dependency for pericardial tissue in human [14]. Miller proposed a three-dimensional hyper-viscoelastic constitutive model for kidney and liver tissue on the basis of in vivo experiments [15]. Gao et al. proposed two new exponential/logarithmic and Ogden based constitutive models for the FE analysis of porcine liver tissue. These models captured the simple tension, compression and pure shear experimental data [16]. Veljkovic et al. investigated the mechanical behavior of porcine aorta under extension-inflation tests using different hyperelastic models. They studied the Fung strain energy function in two dimensions and polyconvex model in three dimensions, concluding that the two-dimensional model had a good agreement with the experimental data, but three-dimensional model did not represent a proper mechanical response in the axial direction of artery [17]. Ogden et al. investigated the mechanical behavior of rubber materials using isotropic stored energy functions in the incompressible state, by the optimization of material parameters with the nonlinear least square analysis [18]. Darijani et al. proposed the novel strain energy functions based on Logarithmic, exponential, power law and polynomial equations. It was shown that the proposed models demonstrated a good agreement with the experimental data [19].

In this research, the nonlinear elastic behavior (Green and Cauchy elastic materials model) of the pericardium of calf and ostrich was investigated. For this purpose, the Cauchy elastic materials were presented as materials with no zero energy in the closed deformation cycle

and the Green elastic materials were introduced with the specific strain energy functions. The coefficients of each constitutive equation were calculated for the best correlation with the experimental data.

2. Nonlinear Elastic Model

In most metals, the elastic part of stress-strain curve is linear, but the elastic behavior is usually nonlinear in polymers, elastomers, and soft tissue. Therefore, a suitable constitutive equation is required to model nonlinear behavior. These constitutive equations are classified into the following two categories: Cauchy and Green elastic materials. These two categories are described in the next sections.

2.1. Cauchy Elastic Materials

In the Cauchy elastic materials, stress does not depend on the history of deformation, but the work done by the stress depends on the deformation path. In these materials, the general form of constitutive equation can be written as [20]:

$$\sigma = H(\mathbf{B}) + \psi_0 \mathbf{I} + \psi_1 \mathbf{B} + \psi_2 \mathbf{B}^2 \quad (1)$$

where α_i s refers to the scalar invariants and \mathbf{I} is the second order identity tensor. By considering the left Cauchy-Green tensor ($\mathbf{B} = \mathbf{V}^2$), Eq. (3) can be rewritten as [20]:

$$\sigma = H(\mathbf{B}) = \psi_0 \mathbf{I} + \psi_1 \mathbf{B} + \psi_2 \mathbf{B}^2 \quad (2)$$

where ψ_0, ψ_1 and ψ_2 are the scalar invariants of \mathbf{B} . Since a tensor should satisfy the characteristic equation, the Cauchy elastic material constitutive equation is written by considering the hydrostatic pressure as a constraint [20]:

$$\sigma = -p \mathbf{I} + \varphi_1 \mathbf{B} + \varphi_2 \mathbf{B}^{-1} \quad (3)$$

In simple tension, $\sigma_1 = \sigma \neq 0$ and $\sigma_2 = \sigma_3 = 0$. If λ_1, λ_2 , and λ_3 represent the principal stretches for incompressible materials in the uniaxial tension, the relation $\lambda_1 = \lambda$ and $\lambda_2 = \lambda_3 = \lambda^{-0.5}$ can be assumed. Therefore, by using Eq. (3) and condition $\sigma_2 = \sigma_3 = 0$, the hydrostatic pressure can be calculated as $p = \frac{\varphi_1}{\lambda} + \varphi_2 \lambda$. Thus, Eq. (3) can be expressed as:

$$\sigma = \left(\lambda^2 - \frac{1}{\lambda} \right) \varphi_1 + \left(\frac{1}{\lambda^2} - \lambda \right) \varphi_2 \quad (4)$$

If a material obeys the Cauchy elastic response, the experimental data should be fitted with the Eq. (4). In the next section, the Green elastic response of material will be discussed.

2.2. Green Elastic Materials

In Green elastic materials (hyperelastic materials), the work does not depend on the deformation path. In

other words, in the Cauchy materials, only the stress is independent of loading path, but in the Green materials, the work is also independent of load path in addition to the stress [25]. These materials are characterized by a strain energy function with necessary conditions [20]. So, according to the material symmetries and strain energy functions conditions [21], it can be written [18,21]:

$$W(\lambda_1, \lambda_2, \lambda_3) = W(\lambda_1) + W(\lambda_2) + W(\lambda_3) \quad (5)$$

As mentioned $\lambda_1 = \lambda$ and $\lambda_2 = \lambda_3 = \lambda^{-0.5}$ for incompressible materials in the uniaxial tension, Eq. (5) can be expressed:

$$W(\lambda) = W(\lambda) + W(\lambda^{-0.5}) + W(\lambda^{-0.5}) \quad (6)$$

The principle Lagrangian stresses are obtained by the derivative of strain energy function with respect to stretches [22, 23, 28]:

$$S_i = \frac{\partial W}{\partial \lambda_i} \quad (7)$$

1. The exponential-exponential function (exp-exp):

$$W(\lambda_i) = \sum_{k=1}^{\infty} A_k [\exp(m_k(\lambda_i - 1)) - 1] + \sum_{k=1}^{\infty} B_k [\exp(n_k(\lambda_i^{-1} - 1)) - 1] \quad (9)$$

2. The exponential-power law function (exp-pow):

$$W(\lambda_i) = \sum_{k=1}^{\infty} A_k [\exp(m_k(\lambda_i - 1)) - 1] + \sum_{k=1}^{\infty} B_k (\lambda_i^{-n_k} - 1) \quad (10)$$

3. The power law-power law function (pow-pow):

$$W(\lambda_i) = \sum_{k=1}^{\infty} A_k (\lambda_i^{m_k} - 1) + \sum_{k=1}^{\infty} B_k (\lambda_i^{-n_k} - 1) \quad (11)$$

where A_k, B_k, m_k and n_k are constants obtained from fitting these equations to the experimental data. Also, λ_i s refers to principal stretches in different directions. It should be noted that there are two summations in the above equations. The first summation provides the positive infinity at the large deformation case and the second one causes the negative infinity at the singularity case.

In this paper, the sum of squared errors (SSE) was used for the description of the accuracy of the models. Actually, SSE represents the difference between the experimental values x_i^{exp} and the modelled (theoretical) values x_i^{theo} . It was calculated as follows:

$$SSE = \sum_{i=1}^n (x_i^{exp} - x_i^{theo})^2 \quad (12)$$

Also, the principle Cauchy stresses can be obtained as [22,23,28]:

$$\sigma_i = \lambda_i \frac{\partial W}{\partial \lambda_i} \quad (8)$$

In Eq. (8), “ i ” is not a dummy index. Many strain energy functions such as Mooney-Rivlin, Ogden, and Neo-Hookean have been used in the recent investigations, but in this study, the robust novel strain energy functions proposed by Darijani and Naghdabadi were used [22]. The following functions, which include power law and exponential terms, satisfy the strain energy function conditions. By combining these functions, 16 strain energy functions can be derived. In this paper, only exponential-exponential (exp-exp), exponential-power law (exp-pow) and power law-power law (pow-pow) strain energy functions have been investigated [22]. Generally, the strain energy function for multiaxial loading can be stated as [22,23]:

3. Results and Discussion

The mechanical behavior of pig, calf, and ostrich pericardium in sutured and unsutured states, with Gore-Tex at 45° and 90°, cut in the dimensions of 12 × 2 cm² was compared with the uniaxial tensile test results obtained by Paez et al. [5]. The stress-strain experimental data of the uniaxial tensile test for ostrich and calf pericardium were adopted from Paez et al. [5]. The experimental stress-strain data of human and canine pericardium with the size 3 × 3 cm² in the uniaxial tensile were adopted from Lee and Boughner [9].

In the Cauchy elastic material response, the stress was calculated from Eq. (4). The coefficients of Eq. (4) and SSE of best fit of Eq. (4) with experimental data were demonstrated in Table 1. The stress-stretch results obtained from Eq. (4) and data of Table 1 have been shown in Fig. 1. As can be seen, the Cauchy

elastic material stress did not fit the uniaxial tensile test data for ostrich, canine and human and only calf pericardium data could be fitted precisely. It should be noted that the range of stress axes in Fig. 1 was not the same for the cases of calf and ostrich. Therefore, as it can be seen in Table 1, the SSE of fitting for the case of ostrich pericardium was higher than that of calf pericardium.

The energy of deformation can be calculated as [19]:

$$W = \int_1^\lambda \frac{\sigma}{\lambda} d\lambda \quad (13)$$

The results of the calculated energy of stress curves, as shown in Fig. 1, could be seen in Fig. 2. Since the coefficients of data fitting were calculated based on the stress-stretch/strain curves of the uniaxial tension tests, there was no guarantee that the energy functions could be fitted to the experimental energy data

with these coefficients. Also, there was no constraint for energy to be non-negative during the deformation. According to Figs. 2b and 2d, it could be seen that not only did the theoretical energy function not fit the experimental data, but also the negative energy was generated in the limiting range of stretches, which was not a physical result. Additionally, there was a poor correlation between the fitted energy curves and the experimental data for other cases.

Table 1
Coefficients of the stress response in the Cauchy elastic materials (Eq. (4)).

Case	φ_1 (MPa)	φ (MPa)	SSE
Calf	56.66	58.88	0.01097
Ostrich	539.4	608.4	235.3
Canine	22.65	22.78	45.44
Human	16.51	18.11	44.17

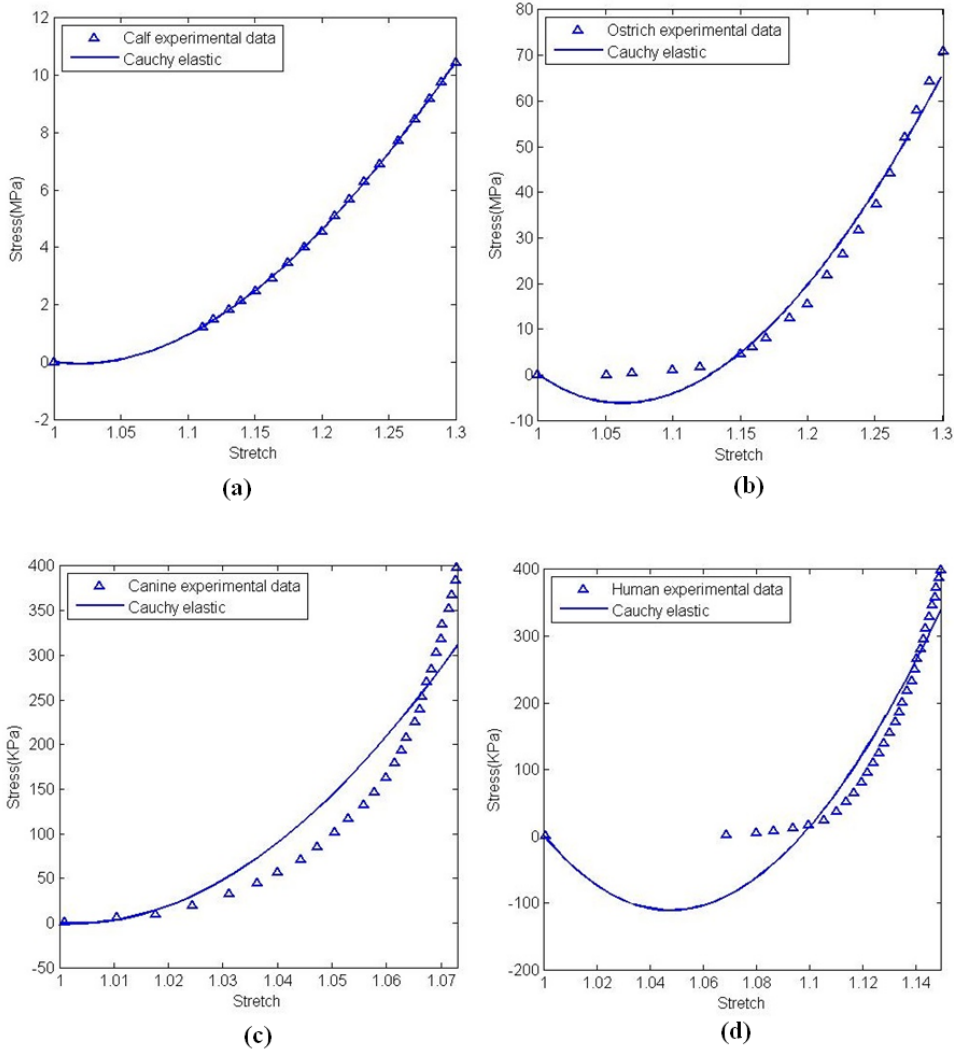


Fig. 1. Stress of Cauchy elastic response and the experimental data: (a) calf pericardium, (b) ostrich pericardium, (c) canine pericardium, and (d) human pericardium.

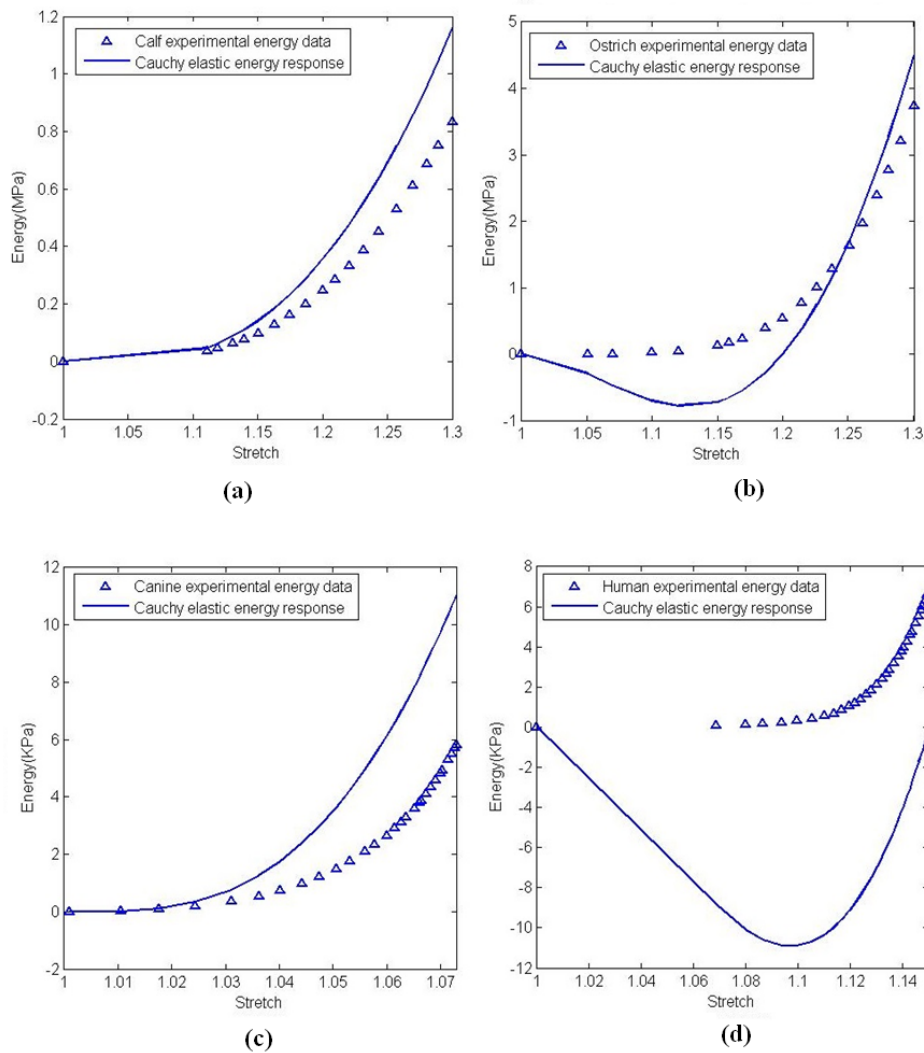


Fig. 2. Energy of Cauchy elastic response and the experimental data: (a) calf pericardium, (b) ostrich pericardium, (c) canine pericardium, and (d) human pericardium.

As the Cauchy elastic material does not ensure that the energy is zero in the close cycle of deformation [22,23], the Green elastic material was investigated here. From the viewpoint of Green elastic materials, the energy was calculated from the tensile stress-elongation curves as the surface under the curve of the experimental data. Then, the strain energy functions of exp-exp, pow-pow and exp-pow were fitted with the experimental data. The results of choosing two terms for each of the series in Eq. (9), (10), and (11) can be seen in Fig. 3. The best fitting coefficients and SSE for human, canine, calf and ostrich in the case of Green elasticity are demonstrated in Table 2. The stress-stretch plots have been presented in Fig. 4, using Eq. (8).

In surgical operations, the soft tissue could be subjected to various modes of loading such as pure shear, biaxial and tension; therefore, coefficients of data fitting according to simple tension should capture the pure shear and biaxial data [16, 22]. In this research, pure shear and biaxial data were not available, but the-

oretical biaxial and pure shear stresses were calculated.

According to Fig. 3, it could be observed that all functions, such as exp-exp, exp-pow and pow-pow functions, covered the uniaxial tension data. Also, it could be deduced that pow-pow function had a minimum value of SSE, as can be seen from Table 2, and it was better than exp-exp and exp-pow functions.

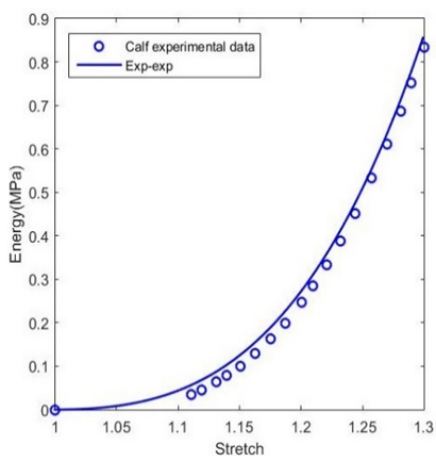
According to Fig. 4, it can be seen for calf and ostrich that the exp-exp, exp-pow and pow-pow energy responses could be fitted with the experimental data. Also, for human and canine, it could be observed that the mentioned stress response covered the experimental data properly. By using the exp-exp, exp-pow and pow-pow energy responses, high values were generated in the biaxial and pure shear modes for calf and ostrich, but in the calf case, the pure shear stress value was obtained to be near the tension value by the exp-exp energy response. Also, in canine, similar to calf, the pure shear curve was sketched to be near the tension curve in the exp-exp energy function.

Table 2
Coefficients of the strain energy functions in the Green elastic materials.

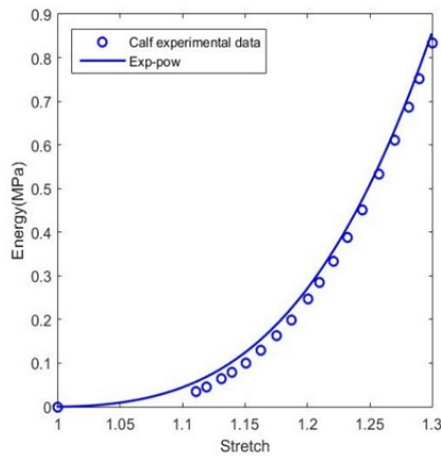
	Calf(exp-exp)	Ostrich(exp-exp)	Canine(exp-exp)	Human(exp-exp)
A_1 (MPa)	0.02275	10.35	-2.015×10^{-3}	-2.639×10^{-3}
A_2 (MPa)	2.539	0.5509	2.004×10^{-3}	1.166×10^{-3}
B_1 (MPa)	0.2031	300.5	1.241×10^{-3}	8.412×10^{-3}
B_2 (MPa)	-20.73	-7670	7.455×10^{-3}	6.771×10^{-3}
m_1 (MPa)	3.122	3.596	5.02×10^{-2}	2.309×10^{-2}
m_2 (MPa)	3.049	7.898	5.111×10^{-2}	2.804×10^{-2}
n_1 (MPa)	7.456	1.847	9.999×10^{-3}	6.378×10^{-3}
n_2 (MPa)	0.9943	0.1937	3.243×10^{-3}	6.223×10^{-3}
SSE	1.848×10^{-4}	0.06649	3.355×10^{-5}	10^{-5}

	Calf(exp-pow)	Ostrich(exp-pow)	Canine(exp-pow)	Human(exp-pow)
A_1 (MPa)	60.77	8.696	3.594×10^{-2}	-3.081×10^{-3}
A_2 (MPa)	75.26	0.3304	1.222×10^{-5}	1.634×10^{-3}
B_1 (MPa)	2.056	49.11	4.446×10^{-3}	1.177×10^{-2}
B_2 (MPa)	-9.154	-4692	-1.286×10^{-2}	3.887×10^{-4}
m_1 (MPa)	0.372	4.725	7.175×10^{-3}	2.364×10^{-2}
m_2 (MPa)	0.3679	0.002812	7.605×10^{-2}	2.75×10^{-2}
n_1 (MPa)	7.963	4.316	3.103×10^{-2}	7.685×10^{-3}
n_2 (MPa)	4.608	0.4916	2.197×10^{-2}	4.236×10^{-4}
SSE	6.413×10^{-5}	0.05812	2.445×10^{-5}	9.955×10^{-6}

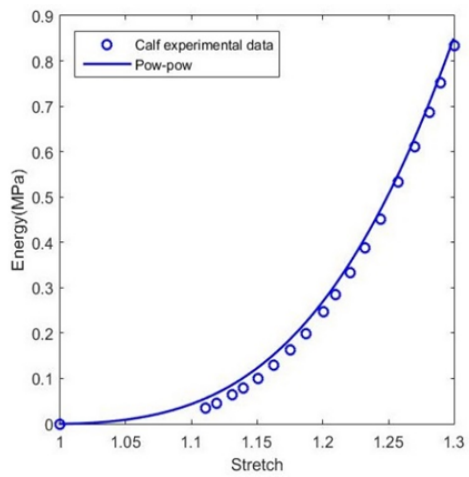
	Calf(pow-pow)	Ostrich(pow-pow)	Canine(pow-pow)	Human(pow-pow)
A_1 (MPa)	66.24	0.2284	-5.25×10^{-3}	-1.185×10^{-3}
A_2 (MPa)	46.94	10	1.742×10^{-3}	4.062×10^{-4}
B_1 (MPa)	3.435	1.622	4.61×10^{-3}	1.126×10^{-2}
B_2 (MPa)	-13.54	-5815	6.528×10^{-2}	4.677×10^{-4}
m_1 (MPa)	0.9189	12.46	2.889×10^{-2}	2.763×10^{-2}
m_2 (MPa)	0.9168	2.167	4.113×10^{-2}	3.493×10^{-2}
n_1 (MPa)	7.335	11.98	9.087×10^{-3}	7.166×10^{-3}
n_2 (MPa)	4.511	0.2263	4.897×10^{-3}	5.677×10^{-4}
SSE	4.55510-5	0.004007	1.372×10^{-5}	9.51×10^{-6}



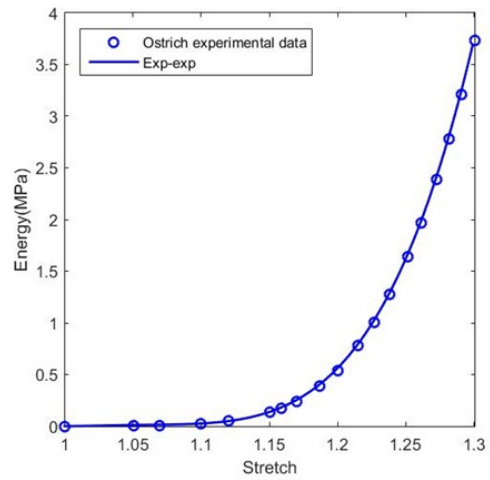
(a)



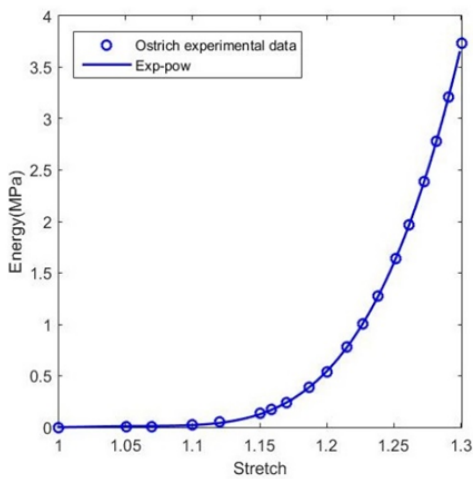
(b)



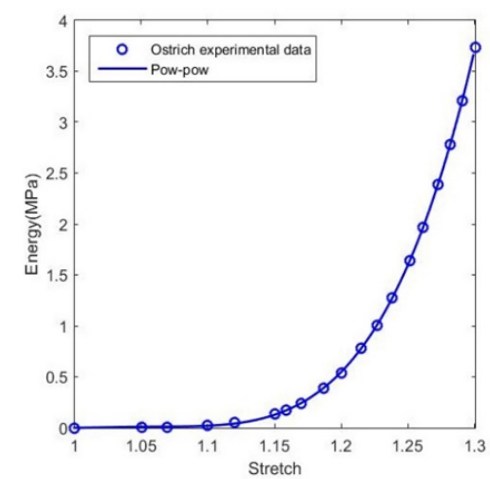
(c)



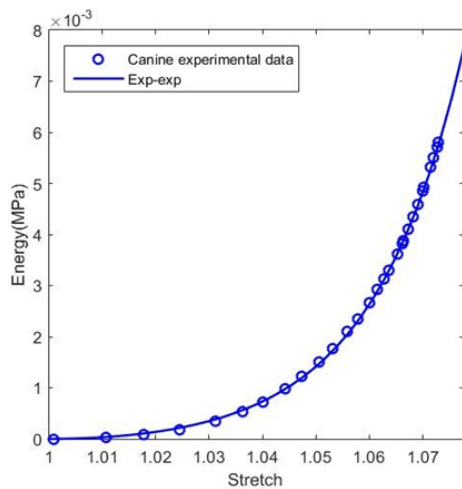
(d)



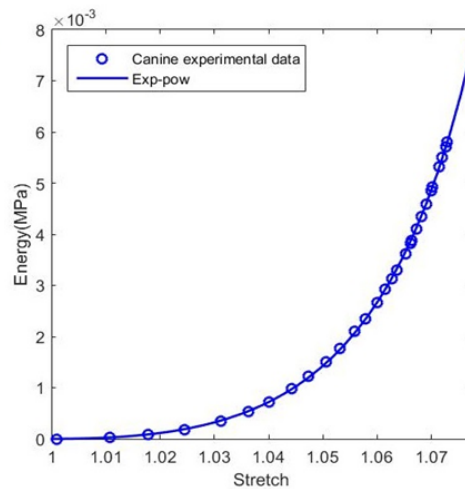
(e)



(f)



(g)



(h)

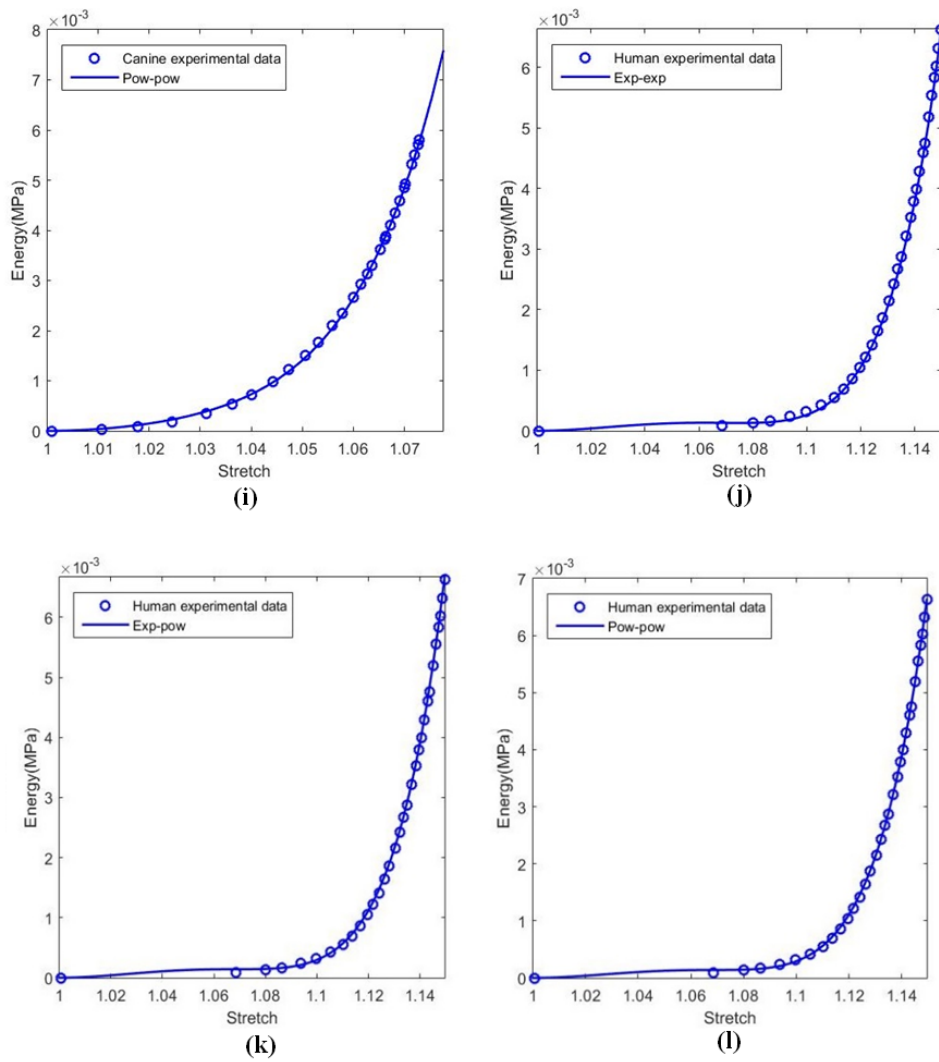
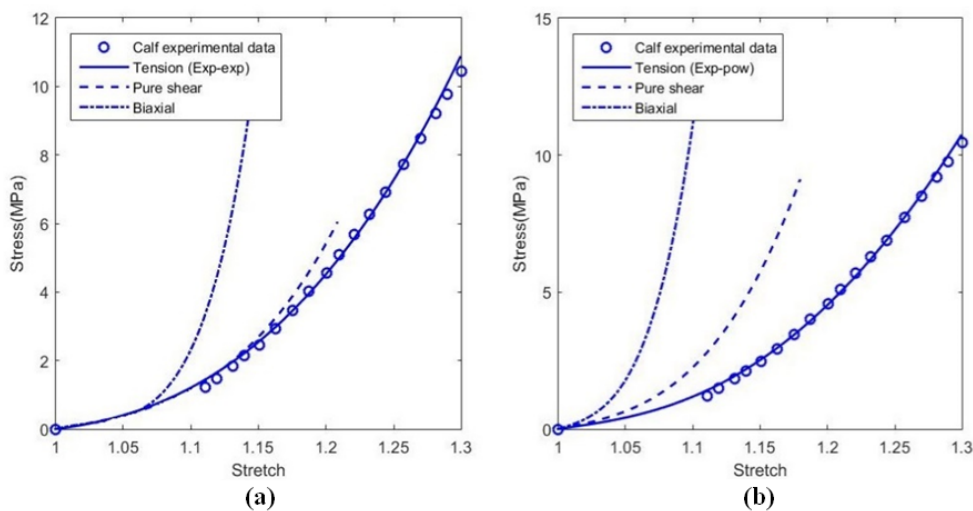
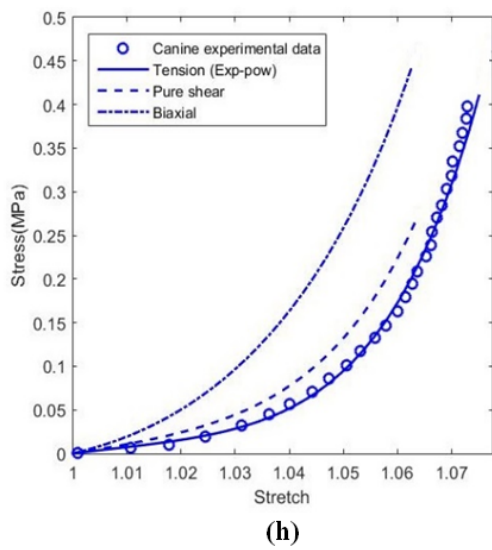
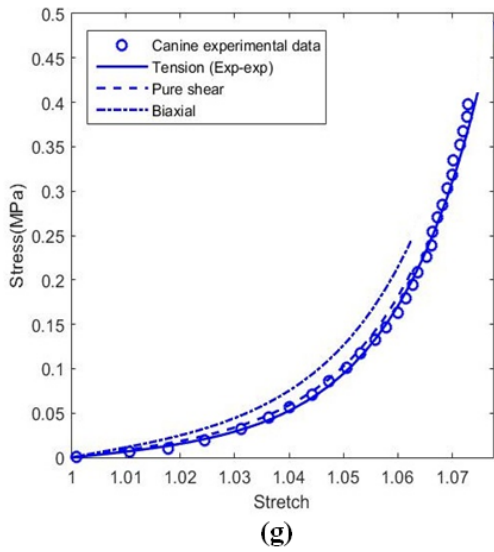
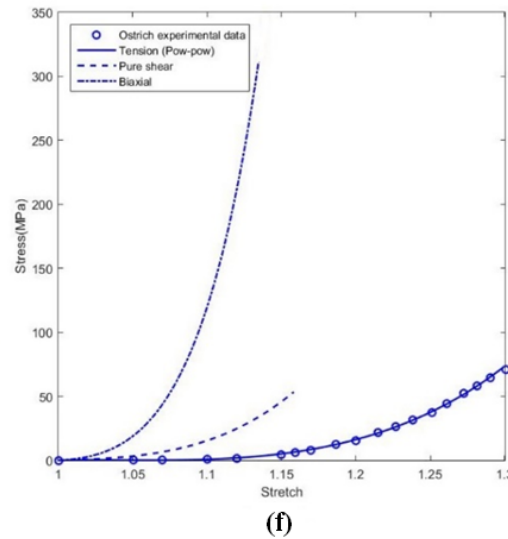
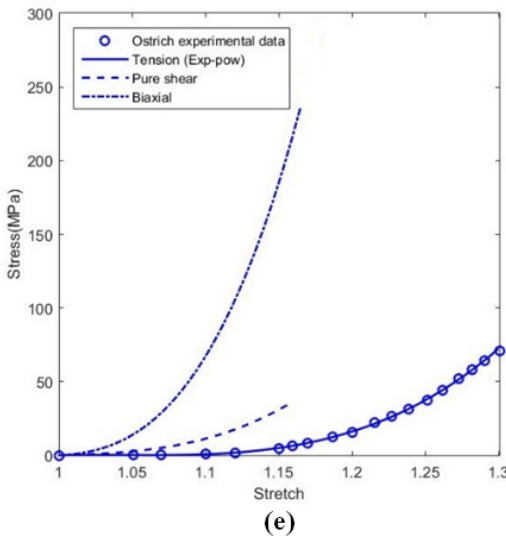
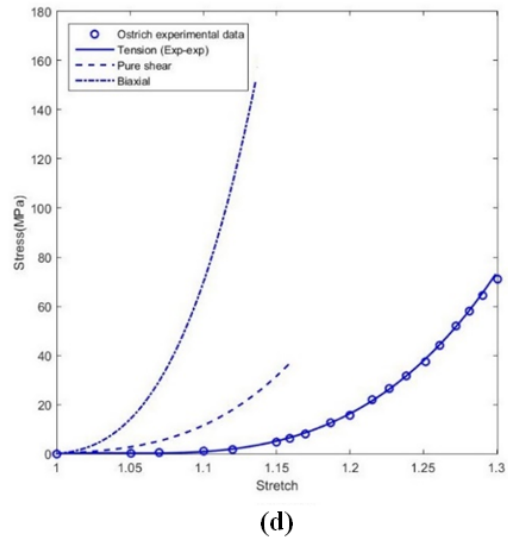
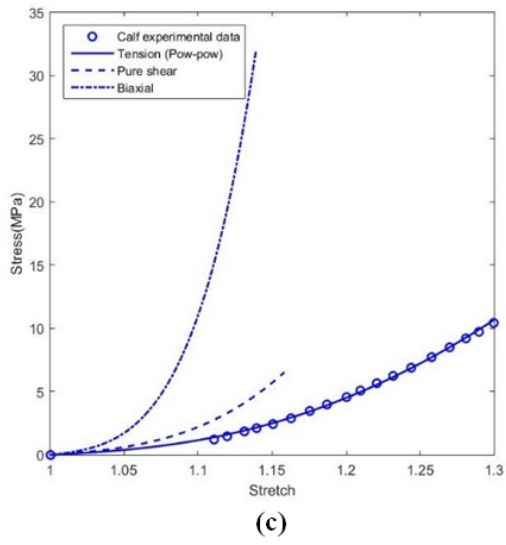


Fig. 3. Experimental energy data and energy-stretch curves of: (a-c) exp-exp, exp-pow and pow-pow stress response of calf pericardium, (d-f) exp-exp, exp-pow and pow-pow stress response of ostrich pericardium, (g-i) exp-exp, exp-pow and pow-pow stress response of canine pericardium, and (j-l) exp-exp, exp-pow and pow-pow stress response of human pericardium.





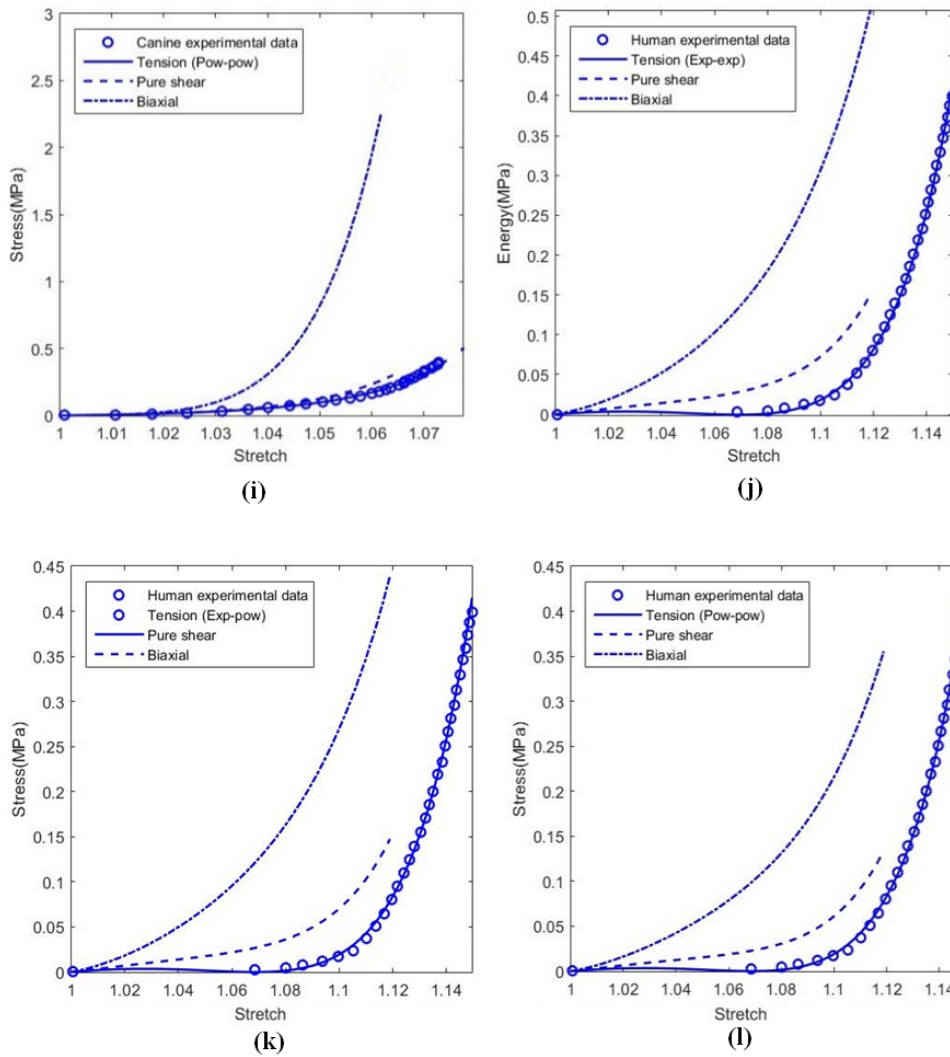


Fig. 4. Experimental data [5,9] and stress-stretch curves of: (a-c) exp-exp, exp-pow, and pow-pow stress response of calf pericardium, (d-f) exp-exp, exp-pow and pow-pow stress response of ostrich pericardium, (g-i) exp-exp, exp-pow and pow-pow stress response of canine pericardium, and (j-l) exp-exp, exp-pow and pow-pow stress response of human pericardium.

It should be noted that the stress response of a nonlinear hyperelastic strain energy is not well-known a priori. Regarding this, in a new hyperelastic strain energy, the stability, sensitivity and stress response in different loading paths and material constants should be investigated [18,26-28]. In this regard, as can be seen in Figs. 3 and 4, the biaxial stress state was different for exp-exp and exp-pow hyperelastic strain energy. Therefore, if there is a new hyperelastic strain energy that represents instability, asymptote or sensitivity with respect to small changes in material constants, the strain energy model should be neglected or modified [26]. Since the modelling of the mechanical behavior of pericardium is important for the design and fabrication of valve leaflets bio-prosthesis, optimization of surgical instruments and development of computer-based simulators for training surgical students [5,24], in a future work, finite element analysis of pericardium

will be studied using a novel hyperelastic constitutive pow-pow equation with the minimum error.

4. Conclusions

In this paper, the mechanical behavior of four types of pericardium, including human, canine, calf, and ostrich pericardium was studied by employing the nonlinear elastic materials theory. At the first step, the Cauchy elastic theory and a nonlinear stress function were discussed. It was shown that the proposed stress function represented an improper accommodation to the experimental stress-strain data in the uniaxial tensile test. Also, the energy function obtained from the integration of stress function did not fit the experimental energy data, producing the residual energy. At the Second step, the Green elastic material behavior was investigated. The strain energy functions of the exp-exp,

pow-pow, and exp-pow equations were obtained in the uniaxial tensile test. It was shown that the calculated energy functions had good fitting with the experimental data. Also, through these functions, the pow-pow energy function had less error than other functions. In general, it was obvious that the Cauchy elastic materials theory could not predict the nonlinear mechanical behavior of pericardium tissue reasonably, as compared to the results of Green elastic materials. Furthermore, since the energy is zero in the Green elastic materials response in a close deformation path, this theory could be utilized in finite element analysis and among the proposed models, the pow-pow model seems to have the minimum error.

5. Acknowledgements

The authors would like to thank K. N. Toosi University of Technology, Tehran, Iran, for providing the financial support and research facilities used in this work.

References

- [1] R.V. Noort, S.P. Yates, T.R.P. Martin, A.T. Barker, M.M. Black, A study of the effects of glutaraldehyde and formaldehyde on the mechanical behaviour of bovine pericardium, *Biomaterials*. (1982) 21-26.
- [2] P.H. Chew, F.S.P. Yin, S.L. Zeger, Biaxial Stress-strain Properties of Canine Pericardium, *J. Mol. Cell. Cardiol.* (1986) 567-578.
- [3] M.M. Maestro, J.O.N. Turnay, P. Fernandez, D. Suarez, J.M.G. Paez, S. Urillo, M.A. Lizarbe, E. Jorge-Herrero, Biochemical and mechanical behavior of ostrich pericardium as a new biomaterial, *Acta. Biomater.* 2 (2006) 213-219.
- [4] E. Daar, E. Woods, J.L. Keddie, A. Nisbet, D. A. Bradley, Effect of penetrating ionising radiation on the mechanical properties of pericardium, *Nucl. Instrum. Methods.* 619 (2010) 356-360.
- [5] J. M.G. Paez, E.J. Herrero, A.C. Sanmartin, I. Millan, A. Cordon, M.M. Maestro, A. Rocha, B. Arenaz, J.L. Castillo-Olivares, Comparison of the mechanical behaviors of biological tissues subjected to uniaxial tensile testing: pig, calf and ostrich pericardium sutured with Gore-Tex, *J. Biomaterials*. 24 (2003) 1671-1679.
- [6] R. Claramunt, J.M.G. Paez, L. Alvarez, A. Ros, M.C. Casado, Fatigue behaviour of young ostrich pericardium, *Mater. Sci. Eng.* (2012) 1415-1420.
- [7] D. Cohn, H. Younes, E. Milgarter, G. Uretzky, Mechanical behaviour of isolated pericardium: species, isotropy, strain rate and collagenase effect on pericardium tissues, *J. Clin. Mater.* (1987) 115-124.
- [8] P. Zioupos, J.C. Barbenel, Mechanics of native bovin pericardium, *J. Biomaterials*. (1994) 374-382.
- [9] J.M. Lee, D.R. Boughner, Mechanical properties of human pericardium. Differences in viscoelastic response when compared with canine pericardium., *Circ. Res.* (1985) 475-481.
- [10] N. Gundiah, M.B. Ratcliffe, L.A. Pruitt, Determination of strain energy function for arterial elastin: Experiments using histology and mechanical tests, *J. Biomech.* (2007) 586-594.
- [11] M.A. Zulliger, P. Fridez, K. Hayashi, N. Stergiopoulos, A strain energy function for arteries accounting for wall composition and structure, *J. Biomech.* (2004) 989-1000.
- [12] M.A. Zulliger, N. Stergiopoulos, Structural strain energy function applied to the ageing of the human aorta, *J. Biomech.* (2007) 3061-3069.
- [13] S.G. Kulkarni, X.L. Gao, S.E. Horner, R.F. Martlock, J.Q. Zheng, A transversely isotropic visco-hyperelastic constitutive model for soft tissues, *Math. Mech. Solids.* (2014) 1-24.
- [14] P.G. Pavan, P. Pachera, C. Tiengo, A. Natali, Biomechanical behavior of pericardial human tissue: a constitutive formulation, *Inst. Mech. Eng. H J. Eng. Med.* (2014) 926-934.
- [15] K. Miller, Constitutive modelling of abdominal organs, *J. Biomech.* (2000) 367-373.
- [16] Z. Gao, K. Lister, D.J. Desai, Constitutive Modeling of Liver Tissue: Experiment and Theory, *Ann. Biomed. Eng.* (2010) 505-516.
- [17] D.Z. Veljkovic, V.J. Rankovic, S.B. Pantovic, M.A. Rosic, M.R. Kojic, Hyperelastic behavior of porcine aorta segment under extension-inflation tests fitted with various phenomenological models, *Acta. Bioeng. Biomech.* (2014) 37-45.
- [18] R.W. Ogden, G. Saccomandi, I. Sgura, Fitting hyperelastic models to experimental data, *Comput. mech.* (2004) 484-502.
- [19] H. Darijani, R. Naghdabadi, M.H. Kargarnovin, Hyperelastic materials modelling using a strain measure consistent with the strain energy postulates, *J. Mech. Eng. Sci.* (2010) 591-602.
- [20] R.W. Ogden, *Nonlinear elastic deformation*, Dover Publication, 1997.
- [21] T. Belytschko, W.K. Liu, B. Moran, *Nonlinear finite elements for continua and structures*, John Wiley and Sons, LTD, 2000.

- [22] H. Darijani, R. Naghdabadi, Hyperelastic materials behavior modeling using consistent strain energy density functions, *Acta. Mech.* (2010) 235-254.
- [23] M. Mansouri, H. Darijani, Constitutive modeling of isotropic hyperelastic material in an exponential framework using a self-contained approach, *Int. J. Solids. Struct.* (2014) 4316-4326.
- [24] F.J. Carter, T.G. Frank, P.J. Davies, D. Mc Lean, A. Cuschieri, Measurements and modelling of the compliance of human and porcine, *Med. Image. Ana.* (2001) 231-236.
- [25] M.W. Lai, E. Krempl, D. Ruben, *Introduction to continuum mechanics*, Elsevier. (2010).
- [26] T. Beda, An approach for hyperelastic model-building and parameters estimation a review of constitutive models, *Eur. Polym. J.* (2004) 97-108.
- [27] A.S. Gendy, A.F. Saleeb, Nonlinear material parameter estimation for characterizing hyperelastic large strain models, *Comput. Mech.* 25 (2000) 66-77.
- [28] H. Hosseinzadeh, M. Ghoreishi, K. Narooei, Investigation of hyperelastic models for nonlinear elastic behavior of demineralized and deproteinized bovine cortical femur bone, *J. Mech. Behav. Biomed. Mater.* 59 (2016) 393-403.